

Adaptive and robust fractional gain based interpolatory cubature Kalman filter

Measurement and Control
1–15

© The Author(s) 2023


Article reuse guidelines:

sagepub.com/journals-permissions

DOI: 10.1177/00202940231200954

journals.sagepub.com/home/mac



Jing Mu¹ , Feng Tian² and Jianlian Cheng³

Abstract

In this study, we put forward the robust fractional gain based interpolatory cubature Kalman filter (FGBICKF) and the adaptive FGBICKF (AFGBICKF) for the development of the state estimators for stochastic nonlinear dynamics system. FGBICKF introduces a fractional gain to interpolatory cubature Kalman filter to increase the robustness of state estimation. AFGBICKF is developed to enhance the state estimation adaptive to stochastic nonlinear dynamics system with unknown process noise covariance through recursive estimation. The simulations on re-entry target tracking system have shown that the performance of FGBICKF is superior to that of cubature Kalman filter and interpolatory cubature Kalman filter, and standard deviation of FGBICKF is closer to posterior Cramér-Rao lower bound. Moreover, our simulations have also demonstrated that AFGBICKF remains stable even when the initial process noise covariance increase, proving its adaptiveness, robustness, and effectiveness on state estimation.

Keywords

Fractional stochastic nonlinear dynamics system, interpolatory cubature rule, adaptive Kalman filter, state estimation

Date received: 24 January 2023; accepted: 24 August 2023

Introduction

Bayesian filtering (BF) has been intensively researched in various applications such as communication, state estimation, and signal processing.¹ Extended Kalman filter (EKF) is a common state estimation algorithms used in the target tracking problem.² However, the implementation of EKF requires computing Jacobian derivative, so EKF may lead to large errors and even divergence in some systems. Then free-derivative Kalman filters were proposed, including unscented Kalman filter (UKF),³ cubature Kalman Filters (CKF),⁴ improved CKF,⁵ robust and adaptive CKF,⁶ interpolatory CKF (ICKF),⁷ the improved central difference Kalman filter,⁸ etc. In the approaches above, the filter gain is achieved by calculating the state covariance and cross covariance between state and measurement. In the course of target tracking, the filter gain lags behind the true state of the target when the target maneuvers, which causes severe tracking errors. So researchers have studied the gain based robust Bayesian filter, such as an optimal control approach to designing constant gain filters,⁹ modified gain EKF,^{10,11} adaptive-gain tracking filters based on minimization of the innovation variance,¹² UKF using modified filter gain,¹³ analysis of the characteristic of the filter gain in

cubature Kalman filter for 1D chaotic maps,¹⁴ and distributed adaptive high-gain EKF.¹⁵

Generally, the prior knowledge of process noise covariance increases the performance of estimation. In practice, however, the prior knowledge of process noise covariance is usually unknown, resulting in model mismatching. Adaptive filtering is an effective method to solve the model mismatching problem. For instance, adaptive Bayesian filters were proposed for unknown process noise covariance, including adaptive Kalman Filtering for dynamic system with outliers,^{16–19} variational Bayesian based Kalman filtering,²⁰ and prior probability statistics based robust estimation algorithm.²¹ These algorithms were developed for the linear and time-invariant systems, assuming prior probability statistics (such as sampling distributions). Some Kalman or extended Kalman based filters were

¹School of Computer Science and Engineering, Xi'an Technological University, Xi'an, China

²Faculty of Science & Technology, Bournemouth University, Poole, UK

³School of Construction Machinery, Chang'an University, Xi'an, China

Corresponding author:

Jing Mu, Xian Technological University, Xuefuzhonglu, Xi'an 710021, China.

Email: mujing@xatu.edu.cn



Creative Commons CC BY: This article is distributed under the terms of the Creative Commons Attribution 4.0 License (<https://creativecommons.org/licenses/by/4.0/>) which permits any use, reproduction and distribution of the work without

further permission provided the original work is attributed as specified on the SAGE and Open Access pages (<https://us.sagepub.com/en-us/nam/open-access-at-sage>).

developed such as ELM based adaptive Kalman filter,²² Kalman filter for dynamic state estimation based on adaptive adjustment of noise covariance,²³ adaptively estimate Q and R based on innovation and residual extended Kalman filter, and sample-based adaptive Kalman filtering for accurate camera pose tracking.²⁴ For specific applications, the adaptive square-root sigma-point Kalman²⁵ and adaptive embedded CKF,²⁶ improved CKF for spacecraft attitude estimation⁵ were proposed. Then the robust Huber-Based Cubature Kalman Filter for GPS Navigation Processing²⁷ was put forward for the non-Gaussian noise. Despite the adaptive filters mentioned above can well address the model mismatching to some extent, they still have limitations such as non-positive covariance matrices and heavy computational load.

Since fractional Kalman filter (FKF) was developed for tracking vehicles,²⁸ quite a few fractional KFs have been proposed recently as fractional calculus gives more accurate results for system analysis. These filters include FCKF for fractional-order nonlinear stochastic systems,²⁹ fractional central difference Kalman filter,³⁰ fractional ICKF,^{31,32} innovation-based fractional adaptive KF,³³ fractional feedback KF for vehicle tracking in video³⁴ and CKF for continuous-time nonlinear fractional-order systems.³⁵

It can be seen from the filters mentioned above that ICKF is practical for state estimation. However, the filter gain in the ICKF is obtained by calculating the covariance of state and cross-covariance between state and measurement, which causes the filter gain to drop behind the target state in rapid change situations. Especially, when the target highly maneuvers, which causes severe tracking error, the tracking performance of the ICKF becomes worse and may diverge. To avoid such divergence, in this paper we put forward the fractional gain based ICKF (FGBICKF), in which the filter gain uses fractional derivative and the gain of the present state depends upon the previous ones. The gain will never be too large, and the FGBICKF performs better even when the target highly maneuvers. Thus, the proposed filter improves the state estimation performance by modifying the filter gain using fractional calculus. Moreover, we take a further step to propose adaptive FGBICKF (AFGBICKF) with recursive estimation of unknown process noise covariance. The simulations on state estimation for re-entry ballistic target (RBT) tracking system have demonstrated the effectiveness and robustness of our proposed filters. The main contributions are summarized in the following:

- We propose FGBICKF, which incorporates fractional derivative of previous filter gains to estimate state of nonlinear systems under Gaussian noise. Meanwhile, we analyze the errors of FGBICKF with posterior Cramér-Rao lower bound (PCRLB).³⁶

- We propose AFGBICKF to enhance FGBICKF for estimation under unknown process noise covariance.
- We conduct the simulation on RBT tracking with FGBICKF and AFGBICKF, and we make errors analysis of FGBICKF using PCRLB. The results show that FGBICKF outperforms CKF and ICKF.
- We analyze the influence of process noise covariance on the performance of AFGBICKF. The simulation results demonstrate AFGBICKF's adaptiveness, robustness, and effectiveness on RBT tracking.

The remainder of this paper is organized as follows. We review some preliminaries on the Grünwald-Letnikov (G-L) fractional difference, Bayesian filtering, and interpolatory cubature rule (ICR) in Section 2. The main algorithms are derived in Section 3, where we first developed FGBICKF by introducing a fractional gain to ICKF, and then put forward AFGBICKF with adaption to unknown process noise covariance using recursive method. In Section 4, we apply the proposed filters to RBT tracking and show the performance of FGBICKF with analysis of its PCRLB. Meanwhile, we present the performance of AFGBICKF and analyze the influence of various process noise covariance on AFGBICKF. Concluding remarks on the results are drawn in Section 5.

Preliminaries

G-L fractional difference

The G-L fractional difference concept can be defined as follows:

$$\Delta^\alpha x_k = \frac{1}{h^\alpha} \sum_{j=0}^k (-1)^j \binom{\alpha}{j} x_{k-j} \quad (1)$$

where Δ is the operator of fractional order system, and $\alpha \in \mathbb{R}$ (\mathbb{R} is the set of real numbers) is fractional difference order. And h (it is considered to be unity in the paper) and k are the sampling interval and the sampling number, respectively. The coefficient $\binom{\alpha}{j}$ can be calculated as:

$$\binom{\alpha}{j} = \begin{cases} 1 & \text{if } j = 0 \\ \frac{\alpha(\alpha-1)\cdots(\alpha-j+1)}{j!} & \text{if } j > 0 \end{cases} \quad (2)$$

Equation (2) is the discrete equivalent of derivative when α is greater than zero.

Bayesian filtering

We consider the stochastic nonlinear dynamics system (SNDS) with additive Gaussian noise, which is

modelled using the following state and the measurement equation:

$$x_k = f(x_{k-1}) + w_{k-1} \quad (3)$$

$$l_k = h(x_k) + v_k \quad (4)$$

where $x_k \in \mathbb{R}^{n_x}$ and $l_k \in \mathbb{R}^{m_l}$ are the state and measurement vector, respectively, f and h are known nonlinear functions; $w_{k-1} \sim N(0, Q_{k-1})$ is Gaussian process noise, and v_k is measurement noise with zero mean and R_k , respectively, w_{k-1} and v_k are mutually uncorrelated noises. $L_{1:k} = \{l_1, l_2, \dots, l_k\}$ is measurement data set obtained by one or more sensors from time step 1 to k .

In the Bayesian filter under Gaussian noise, the complete statistical description of the state (x_k) can be obtained by the posterior density of the state. $\hat{\mu}_{k-1}$ and P_{k-1} are denoted as the state estimation and covariance at time $k-1$, $\hat{\mu}_k$, and P_k as the state estimation and covariance at time k . When a new measurement (l_k) at time k is received, the posterior density $p(x_k|L_k) = N(x_k; \hat{\mu}_k, P_k)$ from the posterior density $p(x_{k-1}|L_{k-1}) = N(x_{k-1}; \hat{\mu}_{k-1}, P_{k-1})$ of the state at time $k-1$ is obtained in two steps:

- (1) Time update, which involves computing the predictive state $\bar{\mu}_k$ and covariance \bar{P}_k :

$$\begin{aligned} \bar{\mu}_k &= E[x_k|L_{k-1}] \\ &= E[f(x_{k-1}) + w_{k-1}|L_{k-1}] = E[f(x_{k-1})|L_{k-1}] \\ &= \int_{\mathbb{R}^{n_x}} f(x_{k-1})p(x_{k-1}|L_{k-1})dx_{k-1} \\ &= \int_{\mathbb{R}^{n_x}} f(x_{k-1}) \times N(x_{k-1}; \hat{\mu}_{k-1}, P_{k-1})dx_{k-1} \end{aligned} \quad (5)$$

$$\begin{aligned} \bar{P}_k &= E[(x_k - \bar{\mu}_k)(x_k - \bar{\mu}_k)^T|L_{1:k}] \\ &= \int_{\mathbb{R}^{n_x}} f(x_{k-1})f(x_{k-1})^T \times N(x_{k-1}; \hat{\mu}_{k-1}, P_{k-1})dx_{k-1} \\ &\quad - \bar{\mu}_k \bar{\mu}_k^T + Q_{k-1} \end{aligned} \quad (6)$$

- (2) Measurement update, which involves computing the measurement prediction \bar{l}_k , innovation covariance $\bar{P}_{ll,k}$, cross covariance $P_{xl,k}$ based on predictive posterior density $x_k \sim N(x_k; \bar{\mu}_k, \bar{P}_k)$ obtained in the time update.

$$\bar{l}_k = \int_{\mathbb{R}^{n_x}} h(x_{k-1}) \times N(x_k; \bar{\mu}_k, \bar{P}_k)dx_k \quad (7)$$

$$\bar{P}_{ll,k} = \int_{\mathbb{R}^{n_x}} h(x_{k-1})h(x_{k-1})^T \times N(x_k; \bar{\mu}_k, \bar{P}_k)dx_k - \bar{l}_k \bar{l}_k^T + R_k \quad (8)$$

$$P_{xl,k} = \int_{\mathbb{R}^{n_x}} x_k h^T(x_k) N(x_k; \bar{\mu}_k, \bar{P}_k) - \bar{\mu}_k \bar{l}_k^T \quad (9)$$

The Kalman gain G_k , estimated state $\hat{\mu}_k$, and covariance P_k at k time instant are calculated as:

$$G_k = P_{xl,k} \bar{P}_{ll,k}^{-1} \quad (10)$$

$$\hat{\mu}_k = \bar{\mu}_k + G_k(l_k - \bar{l}_k) \quad (11)$$

$$P_k = \bar{P}_k - G_k \bar{P}_{ll,k} G_k^T \quad (12)$$

Interpolatory Cubature rule

As can be seen in equations (5)–(9), Gaussian filter can be represented as weighted Gaussian integral under Bayesian framework. The product of a nonlinear function $\tau(x)$ and a Gaussian probability density function (PDF) $N(x; \mathbf{0}, \mathbf{I})$ (\mathbf{I} is identity covariance) is described as:

$$Integral[\tau] = \int \tau(x) N(x; \mathbf{0}, \mathbf{I}) dx \quad (13)$$

where $Integral[\tau]$ is an integration and $\tau(x)$ is an arbitrary non-linear function. $Integral[\tau]$ can be approximated by $\phi^{(m,n)}(\tau)$, which is a $2m+1$ th-degree fully symmetric interpolatory cubature rule (ICR) for a n -dimensional Gaussian weighted integral³⁷:

$$Integral[\tau] \approx \phi^{(m,n)}[\tau] = \sum_{p \in P^{(m,n)}} \varphi_p^{(m,n)} \tau[\lambda] \quad (14)$$

Here, $P^{(m,n)} = \{(p_1, \dots, p_n) | m \geq p_1 \geq \dots \geq p_n \geq 0, |p| \leq m\}$, which denotes a set of all distinct n -partitions of the integers $\{0, 1, \dots, m\}$, $p \in \{0, 1, \dots, m\}$, and $|p| = \sum_{i=1}^n p_i$. λ is defined as a generator composed by $[\lambda_{p_1}, \lambda_{p_2}, \dots, \lambda_{p_n}]$, $\lambda_0 = 0$, and $\lambda_{p_i} \geq 0$. The fully symmetric sum $\tau[\lambda]$ is defined as

$$\tau[\lambda] = \sum_{q \in \Pi_p} \sum_s \tau[s_1 \lambda_{q_1}, s_2 \lambda_{q_2}, \dots, s_n \lambda_{q_n}] \quad (15)$$

where Π_p denotes all distinct permutations of p and the inner sum is taken over all of the sign combinations that occur when $s_i = \pm 1$ for those values of i where $\lambda_{q_i} \neq 0$. The weight $\varphi_p^{(m,n)}$ of generator $[\lambda]$ is given by

$$\varphi_p^{(m,n)} = 2^{-K} \sum_{|k| \leq m-|p|} \prod_{i=1}^n \frac{a_{k_i + p_i}}{\prod_{j=0, j \neq p_i}^{k_i + p_i} (\lambda_{p_i}^2 - \lambda_j^2)} \quad (16)$$

where K is the number of non-zero entries in p and $a_0 = 1$, and a_i is derived as following:

$$a_i = \frac{1}{\sqrt{2\pi}} \int_{-\infty}^{+\infty} e^{-x^2/2} \prod_{j=0}^{i-1} (x^2 - \lambda_j^2) dx \quad (i > 0) \quad (17)$$

The arbitrary degree ICR in equation (14) can be used to numerically compute the Gaussian weighted integrals in Gaussian filters. In this paper, the third-degree ICR ($m = 1$) is used to develop the proposed filters to balance computational load and accuracy. The third-degree ICR corresponds to $p \in \{0, 1\}$ and $|p| = \sum_{i=1}^n p_i, |p| \leq 1$ (i.e. $|p| = 0$ or $|p| = 1$). When $|p| = 0$ and $|p| = 1$, the basic interpolatory cubature points (ICPs) ξ_j and the weights ϖ_j can be calculated from (16) as

$$\xi_j = \begin{cases} [0] & j = 1 \\ \lambda_1 e_j & j = 2, \dots, n+1 \\ -\lambda_1 e_j & j = n+2, \dots, r = 2n+1 \end{cases} \quad (18)$$

$$\varpi_j = \begin{cases} 1 - \frac{n}{\lambda_1^2} & j = 1 \\ \frac{1}{2\lambda_1^2} & j = 2, \dots, r = 2n+1 \end{cases}$$

here, e_i denotes the i th column of a unit matrix.

Using the equation (18), $Integral[\tau]$ can be calculated as:

$$Integral[\tau] \approx \sum_{j=1}^r \varpi_j \tau(\xi_j) \quad (19)$$

Further, we expressed the product of a nonlinear function $\tau(x)$ and a Gaussian PDF $N(x; \hat{\mu}, P)$ as follows³⁸:

$$Integral_N[\tau] = \int \tau(x) N(x; \hat{\mu}, P) dx \quad (20)$$

Using equation (19) and $P = SS^T$, equation (20) can be approximated as⁷:

$$Integral_N[\tau] \approx \sum_{j=1}^r \varpi_j \tau(S\xi_j + \hat{\mu}) \quad (21)$$

Proposed methods

FGBICKF

We assume that the state estimate $\hat{\mu}_{k-1}$ and its corresponding covariance P_{k-1} have been obtained at the time step $k-1$. First, we factorize the covariance $P_{k-1} = S_{k-1} S_{k-1}^T$, evaluate the ICPs using ξ_j defined in equation (18) and propagate the ICPs through nonlinear state equation:

$$X_{j,k-1} = S_{k-1} \xi_j + \hat{\mu}_{k-1} \quad (22)$$

$$X_{j,k}^* = f(X_{j,k-1}) \quad (23)$$

We obtained the state prediction $\bar{\mu}_k$ and the prediction error covariance \bar{P}_k conditioned on measurements

$L_{1:k-1}$ by using the equation (21), $E[w_k] = 0$ and $E(w_k w_k^T) = Q_k$,

$$\bar{\mu}_k = E[x_k | L_{1:k-1}] \approx \sum_{j=1}^r \varpi_j X_{j,k}^* \quad (24)$$

$$\begin{aligned} \bar{P}_k &= E[(\bar{\mu}_k - x_k)(\bar{\mu}_k - x_k)^T | L_{1:k-1}] \\ &= E[(f(x_{k-1}) - f(\hat{\mu}_{k-1}))(f(x_{k-1}) - f(\hat{\mu}_{k-1}))^T | L_{1:k-1}] \\ &\quad + E(w_k w_k^T) \\ &\approx \sum_{j=1}^r \varpi_j [(X_{j,k}^* - \bar{\mu}_k)(X_{j,k}^* - \bar{\mu}_k)^T] + Q_{k-1} \end{aligned} \quad (25)$$

Then, factorize the predicted covariance $\bar{P}_k = \bar{S}_k \bar{S}_k^T$, calculate the predicted cubature points and propagate ICPs as

$$Y_{i,k} = \bar{S}_k \xi_j + \bar{\mu}_k \quad (26)$$

$$Y_{i,k}^* = h(Y_{i,k}) \quad (27)$$

Evaluate the predicted measurement, the cross-covariance and innovation covariance as the following:

$$\bar{l}_k = \sum_{i=1}^r \omega_i Y_{i,k}^* \quad (28)$$

$$\begin{aligned} P_{xl,k} &= E[(x_k - \bar{x}_k)(l_k - (h(\bar{x}_k)))] \\ &\approx \sum_{i=1}^r \varpi_i Y_{i,k} Y_{i,k}^* - \bar{x}_k \bar{l}_k^T \end{aligned} \quad (29)$$

$$\begin{aligned} P_{ll,k} &= E[(l_k - h(\bar{x}_k))(l_k - (h(\bar{x}_k)))^T] \\ &\approx \sum_{i=1}^r \varpi_i Y_{i,k}^* Y_{i,k}^{*T} - \bar{l}_k \bar{l}_k^T + R_k \end{aligned} \quad (30)$$

In the Bayesian filtering, the Kalman gain (G_k) is calculated as:

$$G_k = P_{xl,k} P_{ll,k}^{-1} \quad (31)$$

The filter gain is obtained by calculating the covariance of state and cross-covariance between state and measurement. This may worsen the performance of filters when the target dramatically changes its motion. With a high gain, the filter gives more weight to the measurements and thus follows the target more closely. With a low gain, the filter depends on the model predictions more closely and the state estimation accuracy decreases. To improve the performance of filters, we have proposed the fractional gain which the filter gain of the present state depends upon the previous ones. The filter gain value will never be too large so that the proposed filter is more robust to the change of the target's motion.

Now using the fractional derivative, we define the new filter gain named fractional gain (G_{new}) as:

$$G_{new} = G_k - \sum_{j=1}^k (-1)^j Y_j G_{k-j} \quad (32)$$

where $\Upsilon_j = \text{diag}\left[\binom{\alpha_1}{j}, \dots, \binom{\alpha_{m_l}}{j}\right]$ is fractional order. G_{new} includes previous filter gains using fractional derivative, that is, G_{new} is related to all of the previous gains (1, 2, ..., k time instant) and it means that G_{new} is with k -length memory size.

So, the state estimation and corresponding covariance are

$$\hat{x}_k = \bar{x}_k + G_{new}(l_k - \bar{l}_k) \quad (33)$$

$$P_k = \bar{P}_k - G_{new}P_{ll,k}G_{new}^T \quad (34)$$

Proof of the fractional gain (G_{new}) in equation (32).

The predicted state estimation $\bar{\mu}_k$ is evaluated as

$$\bar{\mu}_k = f(\hat{\mu}_{k-1}) \quad (35)$$

where $\hat{\mu}_{k-1}$ is posteriori estimated state at $k-1$ instant time.

The estimated state $\hat{\mu}_k$ with fractional gain is given as

$$\hat{\mu}_k = \bar{\mu}_k + (G_g + \Delta^\alpha G_k)(l_k - h(\bar{\mu}_k)) \quad (36)$$

Here, G_g is gain variable and $\Delta^\alpha G_k$ is the fractional derivative of the previous filter gain, and it is denoted as:

$$\Delta^\alpha G_k = \sum_{j=1}^k (-1)^j \Upsilon_j G_{k-j} \quad (37)$$

The covariance (P_k) of state is defined as:

$$\begin{aligned} P_k &= E\{(x - \hat{\mu}_k)(x - \hat{\mu}_k)^T\} \\ &= E\{(x - \bar{\mu}_k - (G_g + \Delta^\alpha G_k)(l_k - h(\bar{\mu}_k))) \\ &\quad (x - \bar{\mu}_k - (G_g + \Delta^\alpha G_k)(l_k - h(\bar{\mu}_k)))^T\} \end{aligned} \quad (38)$$

To prove the equation (32), the minimum of a posteriori error covariance has to be obtained in the following:

$$\begin{aligned} G_k &= \arg \min_{G_g} E\{(x - \bar{\mu}_k - (G_g + \Delta^\alpha G_k)(l_k - h(\bar{\mu}_k))) \\ &\quad (x - \bar{\mu}_k - (G_g + \Delta^\alpha G_k)(l_k - h(\bar{\mu}_k)))^T\} \end{aligned} \quad (39)$$

To obtain G_k , we solve the following equation in which the left-hand side is the first derivative of function in equation (39):

$$E[(x - \bar{\mu}_k - (G_g + \Delta^\alpha G_k)(l_k - h(\bar{\mu}_k)))(l_k - h(\bar{\mu}_k))^T] = 0 \quad (40)$$

Reformulating equation (40), we have:

$$\begin{aligned} E[(x - \bar{\mu}_k)(l_k - h(\bar{\mu}_k))^T] \\ - (G_g + \Delta^\alpha G_k)E[(l_k - h(\bar{\mu}_k))(l_k - h(\bar{\mu}_k))^T] = 0 \end{aligned} \quad (41)$$

This yields:

$$\begin{aligned} (G_g + \Delta^\alpha G_k)E[(l_k - h(\bar{\mu}_k))(l_k - h(\bar{\mu}_k))^T] \\ = E[(x - \bar{\mu}_k)(l_k - h(\bar{\mu}_k))^T] \end{aligned} \quad (42)$$

Since $P_{xl,k}$ and $P_{ll,k}$ are defined as

$$P_{xl,k} = E[(x_k - \bar{\mu}_k)(l_k - h(\bar{\mu}_k))^T] \quad (43)$$

$$P_{ll,k} = E[(l_k - h(\bar{\mu}_k))(l_k - h(\bar{\mu}_k))^T] \quad (44)$$

Equation (41) is transformed into

$$(G_g + \Delta^\alpha G_k)P_{ll,k} = P_{xl,k} \quad (45)$$

With equation (35), we have

$$G_{new} = P_{xl,k}P_{ll,k}^{-1} - \Delta^\alpha G_k = G_k - \Delta^\alpha G_k \quad (46)$$

So G_{new} in equation (32) is then derived.

We summarize FGBICKF in Algorithm 1 below.

Algorithm 1. FGBICKF algorithm.

Given the state estimates $\hat{\mu}_0$ and its associated error covariance P_0 at time $k=0$, the state estimation procedure can be recursively implemented as follows.

Initialize parameters: $\hat{\mu}_0, P_0$

For $k = 1, 2, \dots$

Step 1. Time update

Calculate the state prediction $\bar{\mu}_k$ and covariance \bar{P}_k using equations (24) and (25).

Step 2. Measurement update

Step 2.1 Calculate the predicted measurement, the cross-covariance, and innovation covariance using equations (28)–(30)

Step 2.2 Compute the fractional gain

$$G_{new} = G_k - \sum_{j=1}^k (-1)^j \Upsilon_j G_{k-j}$$

Step 2.3 Evaluate the state estimate $\hat{\mu}_k$ and P_k covariance using equations (33) and (34).

End.

Table 1. Computational complexity of each step.

Step	Flops
$\bar{\mu}_k$	$2n_\mu^3 + 7n_\mu^2 + 2(F(n_\mu) + 1)n_\mu + F(n_\mu)$
\bar{P}_k	$2n_\mu^3 + 2n_\mu^2 + 2n_\mu$
\bar{l}_k	$2n_\mu^3 + 7n_\mu^2 + 2(H(n_\mu, m_l) + 1)n_\mu + H(n_\mu, m_l)$
$P_{\mu l, k}$	$4n_\mu^2 m_l + 4n_\mu m_l$
$P_{ll, k}$	$4n_\mu m_l^2 + 5m_l^2$
G_{new}	$M_L n_\mu m_l + m_l^3 + 2n_\mu m_l^2$
$\hat{\mu}_k$	$(2 + M_L)n_\mu m_l + 2n_\mu m_l^2 + n_\mu + m_l^3$
P_k	$2m_l n_\mu^2 + (2m_l^2 - m_l)n_\mu$

Computational complexity

To analyze the numerical complexity of FGBICKF using floating-point operations (flops), we define basic arithmetic operations such as addition, subtraction, multiplication, division, comparison, or square root as one flop.

The number of flops for vector-vector operations, matrix-vector product, and matrix-matrix product are explained in Ref.³⁰ Table 1 lists the specific flops of each step of the FGBICKF. In applications, the memory size (k) is too large as the filters is evaluated recursively, so we select the fixed constant value as memory size. In the paper, we select M_L as the memory size (as in equation (32)) under the guarantee of filters' accuracy. $F(n_\mu)$ and $H(n_\mu, m_l)$ are assumed to be the required flops of two nonlinear functions $f(x_{k-1})$ and $h(x_k)$, respectively. Their exact computational complexity is significant but difficult to evaluate. For FGBICKF we have the total complexity:

$$\begin{aligned}
T_{FGBICKF} = & 6n_\mu^3 + 16n_\mu^2 + 6n_\mu^2 m_l + (2F(n_\mu) \\
& + 2H(n_\mu, m_l) + 7)n_\mu \\
& + (5 + M_L + M_L m_l)n_\mu + 10m_l^2 n_\mu \\
& + F(n_\mu) + H(n_\mu, m_l) + 5m_l^2 + 2m_l^3
\end{aligned} \quad (47)$$

The numerical complexity of FGBICKF is $\max\{O(n_\mu^3), O(m_l^3), O(n_\mu F(n_\mu)), O(n_\mu H(m_l, n_\mu))\}$.

Adaptive FGBICKF (AFGBICKF)

In practice, the covariance of the process noise is not usually available as described in equation (3), so we develop a recursive estimation strategy based on covariance matching principle.³⁹

Rewrite equation (25):

$$\bar{P}_k \approx P_{xx, k} + Q_{k-1} \quad (48)$$

Here, $P_{xx, k} = \sum_{j=1}^r \varpi_j [(X_{i, k}^* - \bar{\mu}_k)(X_{i, k}^* - \bar{\mu}_k)^T]$.

Given one-step prediction of state $\bar{\mu}_k$ at time $k-1$ and the estimate state $\hat{\mu}_k$ at time k , the residual between them can be represented by:

$$\zeta_k = \hat{\mu}_k - \bar{\mu}_k \quad (49)$$

Given the residual data from time $k - M_Q + 1$ (M_Q is an adjustable parameter) to time k , the mean and the covariance of ζ_k can be estimated by

$$\bar{\zeta}_k = \frac{1}{M_Q} \sum_{j=k-M_Q+1}^k \zeta_j \quad (50)$$

$$\sum_{\zeta_k} = \frac{1}{M_Q - 1} \sum_{j=k-M_Q+1}^k (\zeta_j - \bar{\zeta}_k)(\zeta_j - \bar{\zeta}_k)^T \quad (51)$$

Provided that the covariance of process noise stays constant, the expectation of equation (51) is given by:

$$E\left(\sum_{\zeta_k}\right) = \frac{1}{M_Q} \sum_{j=k-M_Q+1}^k (P_{xx, j} - P_j) + Q_k \quad (52)$$

By combining equations (51) and (52), the covariance of process noise can be approximately calculated by

$$\begin{aligned}
\hat{Q}_k = & \frac{1}{M_Q - 1} \sum_{j=k-M_Q+1}^k (\zeta_i - \bar{\zeta}_k)(\zeta_i - \bar{\zeta}_k)^T \\
& - \frac{1}{M_Q} \sum_{j=k-M_Q+1}^k (P_{xx, j} - P_j)
\end{aligned} \quad (53)$$

Similarly, Q_{k-1} can be computed as

$$\begin{aligned}
\hat{Q}_{k-1} = & \frac{1}{M_Q - 2} \sum_{j=k-M_Q+1}^{k-1} (\zeta_i - \bar{\zeta}_k)(\zeta_i - \bar{\zeta}_k)^T \\
& - \frac{1}{M_Q - 1} \sum_{j=k-M_Q+1}^k (P_{xx, j} - P_j)
\end{aligned} \quad (54)$$

Through simple mathematical manipulations, equation (53) can be rewritten as the following form

$$\hat{Q}_k = \frac{M_Q - 1}{M_Q} W_k + \Delta Q_k \quad (55)$$

where

$$\begin{aligned}
W_k = & \frac{M_Q}{(M_Q - 1)^2} \sum_{j=k-M_Q+1}^{k-1} \\
& (\zeta_i - \bar{\zeta}_k)(\zeta_i - \bar{\zeta}_k)^T - \frac{1}{M_Q - 1} \sum_{j=k-M_Q+1}^k (P_{xx, j} - P_j)
\end{aligned} \quad (56)$$

Algorithm 2. AFGBICKF algorithm.

Initialize $\hat{\mu}_0, P_0, \hat{Q}_0, M_Q$.

For $k = 1, 2, \dots$

Step 1. Time Update

Calculate the predicted state $\bar{\mu}_k$ and covariance \bar{P}_k , using equations (24) and (25).

Step 2. Measurement update.

Step 2.1 Evaluate the predicted measurement estimate, square root of the cross-covariance, and innovation covariance, using equations (28)–(30).

Step 2.2 Evaluate the modified gain G_{new} using equation (32), state estimate $\hat{\mu}_k$ and covariance P_k using equations (33) and (34).

Step 3. Estimate the process noise covariance recursively.

$\hat{Q}_k = (M_Q - 1)\hat{Q}_{k-1}/M_Q + \Delta Q_k$

where ΔQ_k is defined as equation (58).

End.

If M_Q is large enough, the difference between $M_Q/(M_Q - 1)^2$ and $1/(M_Q - 2)$ is negligible. We set $M_Q = 10$ according to the Remark 4 in the reference Jiang and Cai.³⁹ So, W_k can be approximated as

$$W_k \approx \frac{1}{M_Q - 2} \sum_{i=k-M_Q+1}^{k-1} (\zeta_j - \bar{\zeta}_k)(\zeta_j - \bar{\zeta}_k)^T - \frac{1}{M_Q - 1} \sum_{j=k-M_Q+1}^k (P_{xx,j} - P_j) \quad (57)$$

and

$$\Delta Q_k = \frac{1}{M_Q - 1} (\zeta_k - \bar{\zeta}_k)(\zeta_k - \bar{\zeta}_k)^T - \frac{1}{M_Q} (P_{xx,k} - P_k) \quad (58)$$

Obviously, the above equation has the equivalent form with Q_{k-1} ; therefore, equation (55) can be deduced. Similarly, the recursive estimation equation of ζ_k is given by:

$$\bar{\zeta}_k = \frac{M_Q - 1}{M_Q} \bar{\zeta}_{k-1} + \frac{1}{M_Q} \zeta_k \quad (59)$$

So, we can use equations (49), (55), (56), and (59) to update the covariance of process noise. Provided that the covariance of process noise stays constant, the recursive relation between Q_{k-1} and Q_k can then be described as:

$$\hat{Q}_k = \frac{M_Q - 1}{M_Q} \hat{Q}_{k-1} + \Delta Q_k \quad (60)$$

AFGBICKF algorithm is formulated in the Algorithm 2.

Case study: Re-entry ballistic target tracking

In the following, we apply the proposed FGBICKF and AFGBICKF algorithm to the RBT tracking.⁴⁰ Firstly, the effect of fractional order on FGBICKF is

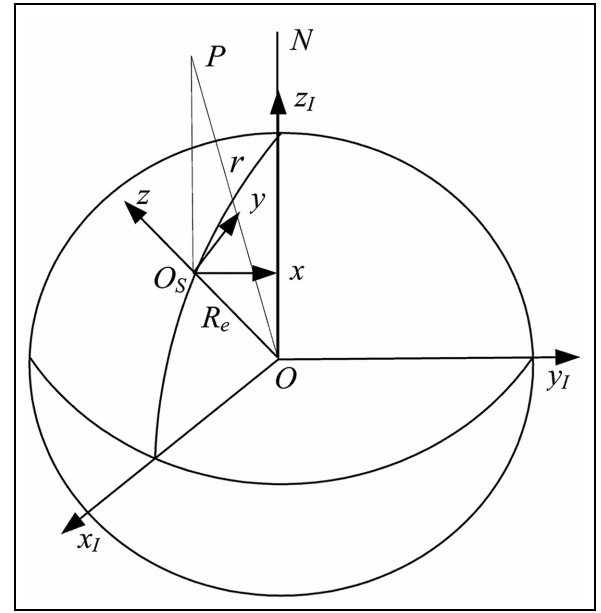


Figure 1. Geometry of radar and RBT (the ECI-CS ($Ox_Iy_Iz_I$) and ENU-CS (O_sxyz)).

analyzed. Then we compare FGBICKF with CKF and ICKF. Furthermore, we compare the standard deviation (STD) of FGBICKF with PCRLB and analyze errors from FGBICKF. Afterwards, we compare AFGBICKF with FGBICKF, while analyzing the influence of various initial process noise covariance on the performance of AFGBICKF algorithm.

RBT dynamics model

Figure 1 shows the geometry of the RBT. P is re-entry ballistic target and the radar is situated at the surface of Earth. The two coordinate systems: the Earth-centered inertial coordinate system (ECI-CS, $Ox_Iy_Iz_I$) and East-North-Up coordinates system (ENU-CS, O_sxyz) are presented in the Figure 1. The ECI-CS is a right-handed system with the origin O at Earth's center, Ox_I pointing to the vernal equinox direction, and the axis Oz_I pointing to the direction of the North Pole N . Its fundamental plane Ox_Iy_I coincides with Earth's equatorial plane. The ENU-CS has its origin at the location

of the radar, and z is directed along the local vertical. x and y lie in a local horizontal plane, x pointing to the east, and y pointing to the north, respectively.

In order to obtain the state equation, we make two hypotheses: one is that Earth is spherical and non-rotating, and another is that only the gravity and drag are the forces acting on the RBT.⁴⁰ According to the transformation relationship of ECI-CS and ENU-CS, we derive the kinematics of the RBT with unknown ballistic coefficient in the ENU-CS. And we model the discrete-time stochastic nonlinear state equation of RBT:

$$\eta_k = \Phi\eta_{k-1} + \Gamma\Psi(\eta_{k-1}) + w_{k-1} \quad (61)$$

here, $\eta_k = [x_k \ vx_k \ y_k \ vy_k \ z_k \ vz_k \ \beta_k]^T$ is the RBT's state, β_k (kg/m^2) is ballistic coefficient, Φ and Γ are described in the following:

$$\Phi = \begin{bmatrix} \delta & 0 & 0 & 0 \\ 0 & \delta & 0 & 0 \\ 0 & 0 & \delta & 0 \\ 0 & 0 & 0 & 1 \end{bmatrix}, \delta = \begin{bmatrix} 1 & t \\ 0 & 1 \end{bmatrix}, \quad (62)$$

$$\Gamma = \begin{bmatrix} \kappa & 0 & 0 \\ 0 & \kappa & 0 \\ 0 & 0 & \kappa \\ 0 & 0 & 0 \end{bmatrix}, \kappa = \begin{bmatrix} t^2/2 \\ t \end{bmatrix},$$

$$\Psi(\eta_{k-1}) = \begin{bmatrix} -\frac{\rho(h_{k-1})}{2\beta_{k-1}} V_{k-1} vx_{k-1} - \frac{\mu x_{k-1}}{r_{k-1}^3} \\ -\frac{\rho(h_{k-1})}{2\beta_{k-1}} V_{k-1} vy_{k-1} - \frac{\mu y_{k-1}}{r_{k-1}^3} \\ -\frac{\rho(h_{k-1})}{2\beta_{k-1}} V_{k-1} vz_{k-1} - \frac{\mu(z_{k-1} + R_e)}{r_{k-1}^3} \end{bmatrix} \quad (63)$$

Here t (in second, i.e. s) is the time interval between radar measurements, $\mu = 3.986005 \times 10^{14} \text{m}^3/\text{s}^2$ and $R_e = 6371004 \text{m}$ are Earth's gravitational constant and Earth radius, respectively. And $r_{k-1} = \sqrt{x_{k-1}^2 + y_{k-1}^2 + (z_{k-1} + R_e)^2}$, $V_{k-1} = \sqrt{vx_{k-1}^2 + vy_{k-1}^2 + vz_{k-1}^2}$, and $h_{k-1} = r_{k-1} - R_e$. $\rho(h)$ (kg/m^3) is the air density, which can be approximately modeled as $\rho = c_1 e^{-c_2 h}$ at height below 90 km (c_1, c_2 are dimensionless and constant).⁴¹ w_k is Gaussian noise with zero mean and covariance matrix (Q_k)⁴²:

$$Q_k = \begin{bmatrix} q_1 \vartheta & 0 & 0 & 0 \\ 0 & q_1 \vartheta & 0 & 0 \\ 0 & 0 & q_1 \vartheta & 0 \\ 0 & 0 & 0 & q_2 t \end{bmatrix}, \vartheta = \begin{bmatrix} t^3/3 & t^2/2 \\ t^2/2 & t \end{bmatrix} \quad (64)$$

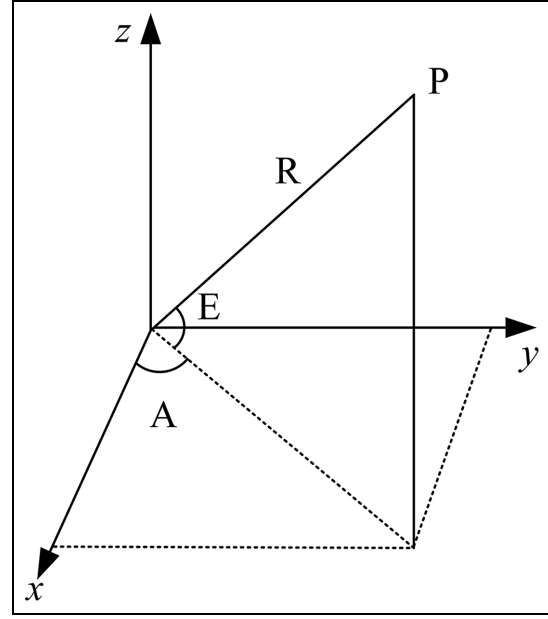


Figure 2. Range (R), elevation (E), and azimuth (A) collected by radar.

Here q_1 (in m^2/s^2) and q_2 (in $\text{kg}^2/(\text{m}^4 \text{s})$) control the amount of process noise and RBT's ballistic coefficient, respectively.

The radar collects the measurements: the range (R), elevation (E), and azimuth (A), which are presented in Figure 2.

The measurement equation in ENU-CS is depicted as follows:

$$l_k = h(x_k) + v_k \quad (65)$$

where $l_k = [R_k E_k A_k]^T$, $h(x_k) = \begin{bmatrix} \sqrt{x_k^2 + y_k^2 + z_k^2} \\ \arctan z_k / \sqrt{x_k^2 + y_k^2} \\ \arctan y_k / x_k \end{bmatrix}^T$. The range R_k , elevation E_k , and azimuth A_k at time instant k are defined: $R_k = \sqrt{x_k^2 + y_k^2 + z_k^2} + v_R$, $E_k = \arctan z_k / \sqrt{x_k^2 + y_k^2} + v_E$, $A_k = \arctan y_k / x_k + v_A$. The measurement noise $v_k = [v_R \ v_E \ v_A]^T$ is the white Gaussian noise, which is with the zero-mean and the covariance matrix $N_k = \text{diag}([\sigma_R^2 \ \sigma_E^2 \ \sigma_A^2])$, σ_R , σ_E , and σ_A are the standard deviations of range, elevation, and azimuth, respectively.

To evaluate the performance of the proposed filters, we use the performance metrics: root mean-square error (RMSE) and average accumulated mean-square root error (AMSRE).⁴³ The RMSE and AMSRE in position at k time instant are defined as follows:

$$\text{RMSE}_p(k) = \frac{1}{M_t} \sum_{i=1}^{M_t} \sqrt{(x_k^{(i)} - \hat{x}_k^{(i)})^2 + (y_k^{(i)} - \hat{y}_k^{(i)})^2 + (z_k^{(i)} - \hat{z}_k^{(i)})^2} \quad (66)$$

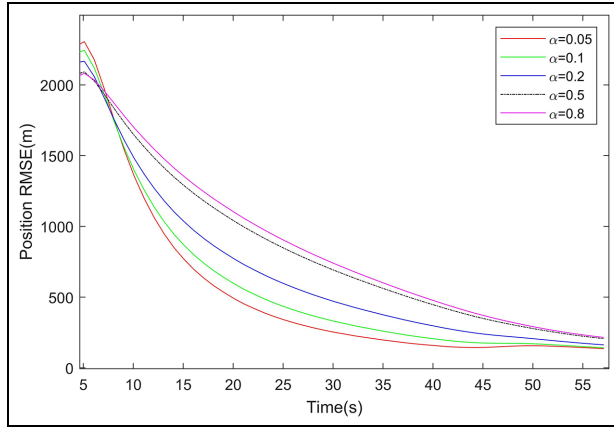


Figure 3. RMSE of FGBICKF for various values of α in position.

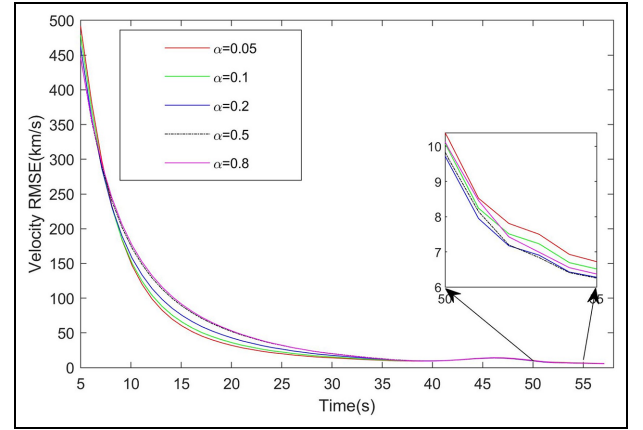


Figure 4. RMSE of FGBICKF for various values of α in velocity.

$$AMSRE_p = \frac{1}{N_t} \sum_{i=1}^{N_t} \sqrt{\frac{1}{M_t} \sum_{k=1}^{M_t} (x_k^{(i)} - \hat{x}_k^{(i)})^2 + (y_k^{(i)} - \hat{y}_k^{(i)})^2 + (z_k^{(i)} - \hat{z}_k^{(i)})^2} \quad (67)$$

Here $(x^{(i)}, y^{(i)}, z^{(i)})$ and $(\hat{x}^{(i)}, \hat{y}^{(i)}, \hat{z}^{(i)})$ are the true and estimated position at the i th Monte Carlo run, M_t is the total Monte Carlo runs, and N_t is the total number of measurement data points. Similarly, we can obtain RMSE and AMSRE in velocity and ballistic coefficient. The obtained RMSEs and AMSREs in the position, velocity and ballistic coefficient in this paper were averaged over 100 independent Monte Carlo runs.

Simulations and analysis

Influence of fractional difference order (α) on FGBICKF. In the simulation, we set the parameters λ_1 , T , q_1 , and q_2 as 2, 0.1 s, $5 \text{ m}^2/\text{s}^3$, and $5 \text{ kg}^2/(\text{m}^4\text{s})$. We initialize the position x_0 , y_0 , and z_0 as 232, 232, and 90 km and module of the velocity v_0 as 3000 m/s. We select the initial elevation E_0 , azimuth angle A_0 and initial ballistic coefficient β_0 as 210° , 45° , and $4000 \text{ kg}/\text{m}^2$. Then the true initial state $x_0 = [232 \text{ km} - 1837 \text{ m/s}, 232 \text{ km} - 1837 \text{ m/s}, 90 \text{ km} - 1500 \text{ m/s}, 4000 \text{ kg}/\text{m}^2]^T$ is obtained, and the covariance $P_0 = \text{diag}([100^2 \ 50^2 \ 100^2 \ 50^2 \ 100^2 \ 50^2 \ 200^2])$ is set. The initial state estimate is randomly chosen from $\hat{x}_0 \sim \mathcal{N}(x_0, P_0)$. we set the standard deviations of the range errors (σ_R) as 100 m, the elevation angle (σ_E), azimuth angle (σ_A) as 0.017 rad.

In the FGBICKF, the Kalman gain is modified with fractional gain. We have done experiments and found that FGBICKF converged when α was less than 1 ($\alpha < 1$). The simulation is carried out by selecting the fractional order α as 0.05, 0.1, 0.2, 0.5, and 0.8, respectively. Figures 3 to 5 presents the RMSEs of FGBICKF with various fractional orders for the position, the velocity, and the ballistic coefficient.

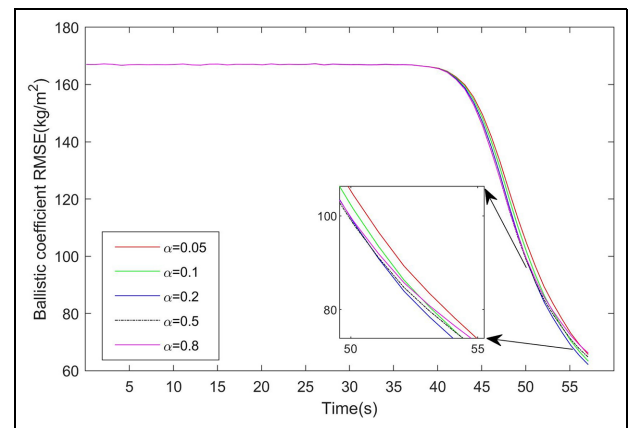


Figure 5. RMSE of FGBICKF for various values of α in ballistic coefficient.

As can be seen from Figures 3 to 5, FGBICKF clearly converges. It is observed that there is a tradeoff between convergence rate and estimation accuracy from RMSEs in position, velocity, and ballistic coefficient. For $\alpha = 0.1$, the RMSE of FGBICKF in the position is lower than that of other values of α except $\alpha = 0.05$, and the RMSE of FGBICKF in the velocity is lower than that of other values of α except $\alpha = 0.05$ before the estimation time 50 s. The RMSE of FGBICKF in the ballistic coefficient is higher than that of other values of α except $\alpha = 0.05$ after the estimation time 50 s. It has been shown that FGBICKF has better performance when the fractional order is set as $\alpha = 0.1$.

Comparison of FGBICKF and CKF, ICKF. In the subsection, we compare the performance of FGBICKF with fractional order $\alpha = 0.1$ with that of CKF and ICKF when they are applied to state estimation in the RBT tracking problem. Here, the values of the parameters (λ_1 , \hat{x}_0 , P_0 , Q_k , and R_k) are set the same as those in the first subsection. Figures 6 to 8 present RMSEs in position, velocity, and the ballistic coefficient for FGBICKF, CKF, and ICKF.

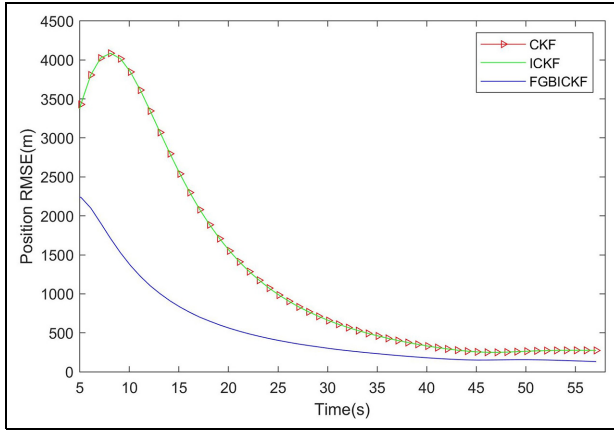


Figure 6. RMSEs in position for various filters.

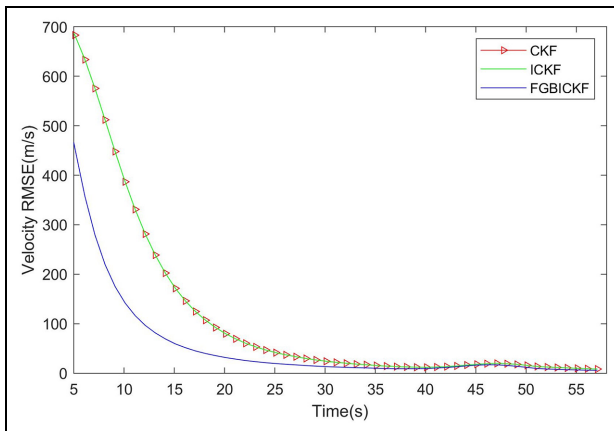


Figure 7. RMSEs in velocity for various filters.

Obviously, in terms of effectiveness, Figure 6 to 8 show the high accuracy of FGBICKF, compared with CKF and ICKF. Particularly, Figure 8 illustrates that the estimates of FGBICKF in ballistic coefficient are more accurate than those of CKF and ICKF after 40 s. In FGBICKF, the Kalman gain is modified with fractional characteristics. The information of variations in the previous gain is used to evaluate the next state with the help of fractional derivative. Modified gain gives the better performance for state estimation. From Figures 6 to 8, we can also see that CKF and ICKF achieves mostly the same level of estimation performance in position, velocity, and ballistic coefficient.

Moreover, the runtimes of UKF, CKF, ICKF, and FGBICKF are about 0.76066, 0.24731, 0.26729, and 0.36222 s, respectively. We see the runtime of FGBICKF is less than that of UKF due to its requirement for computing sigma points, and FGBICKF has a slightly higher computational complexity, compared to CKF and ICKF. FGBICKF is slightly slower due to its requirements on evaluating more past gain.

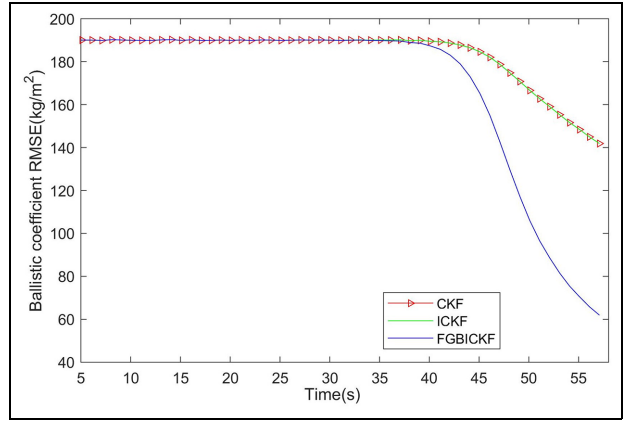


Figure 8. RMSEs in ballistic coefficient for various filters.

Error analysis on FGBICKF. Cramér-Rao lower bound (CRLB) provides the best error analysis for filter and is used to evaluate the performance of filters.⁴⁴ $CRLB_k$ (i.e. CRLB at k time instant) is defined as:

$$CRLB_k = J_k^{-1} \quad (68)$$

where J_k is the fisher information matrix and is defined as

$$J_k = E \left[-\frac{\partial^2 \ln p(x_{1:k}, l_{1:k})}{\partial x_k^2} \right] \quad (69)$$

Here, the posterior distribution function of $x_{1:k}, l_{1:k}$ is $p(x_{1:k}, l_{1:k})$. In practice, J_k in equation (69) is hard to be calculated, so we use posterior Fisher information matrix J_k , which is calculated using the recursive form in equation (70) to obtain the posterior CRLB (PCRLB).³⁶

$$J_{k+1} = D_k^{22} - D_k^{21} [D_k^{11} + J_k]^{-1} D_k^{12} \quad (70)$$

Here, D_k^{11} , D_k^{12} , D_k^{21} , and D_k^{22} are defined as:

$$D_k^{11} = E \left\{ -\frac{\partial^2 \ln p(x_k | x_{k-1})}{\partial^2 x_{k-1}^2} \right\} \quad (71)$$

$$D_k^{12} = (D_k^{21})^T = E \left\{ -\frac{\partial^2 \ln p(x_k | x_{k-1})}{\partial x_{k-1} \partial x_k} \right\} \quad (72)$$

$$D_k^{22} = E \left\{ -\frac{\partial^2 \ln p(x_k | x_{k-1})}{\partial^2 x_k^2} \right\} \quad (73)$$

For nonlinear system with additive Gaussian noise in equations (3) and (4), D_k^{11} , D_k^{12} , D_k^{21} , and D_k^{22} are calculated as

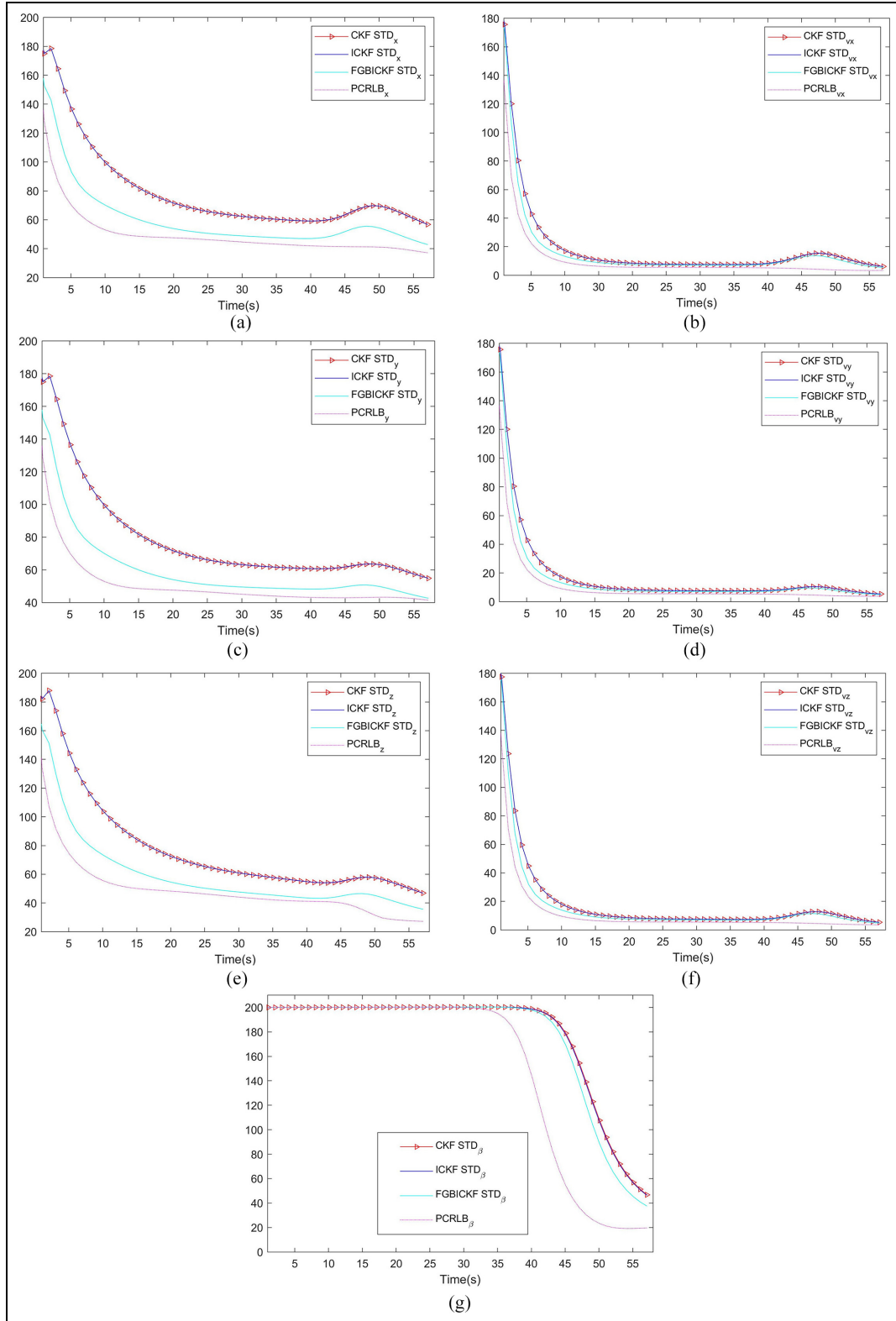


Figure 9. Comparison of STD of various filters and PCRLB: (a) x-axis position, (b) x-axis velocity, (c) y-axis position, (d) y-axis velocity, (e) z-axis position, (f) z-axis velocity, and (g) ballistic coefficient.

$$D_k^{11} = E\{[\nabla_{x_k} f^T(x_k)] Q_k^{-1} [\nabla_{x_k} f^T(x_k)]^T\} \quad (74)$$

$$D_k^{21} = (D_k^{12})^T \quad (76)$$

$$D_k^{12} = -E\{\nabla_{x_k} f^T(x_k)\} Q_k^{-1} \quad (75)$$

$$D_k^{22} = Q_k^{-1} + E\{[\nabla_{x_{k+1}} h^T(x_{k+1})] R_{k+1}^{-1} [\nabla_{x_{k+1}} h^T(x_{k+1})]^T\} \quad (77)$$

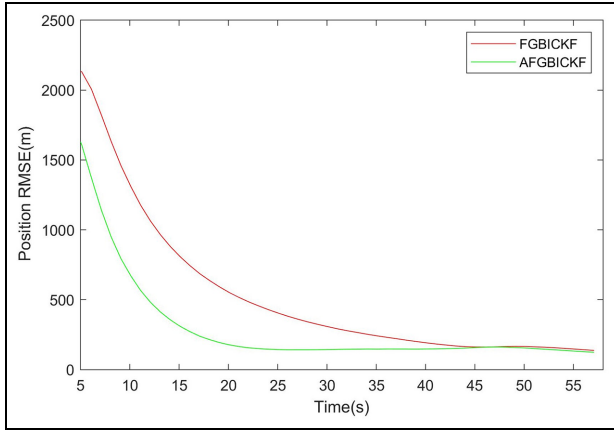


Figure 10. RMSEs in position for FGBICKF and AFGBICKF.

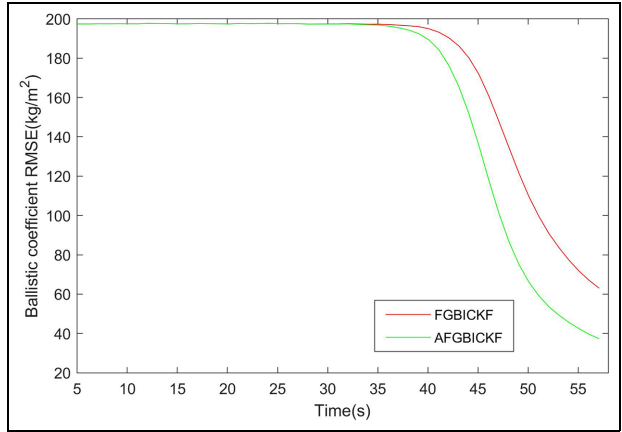


Figure 12. RMSEs in ballistic coefficient for FGBICKF and AFGBICKF.

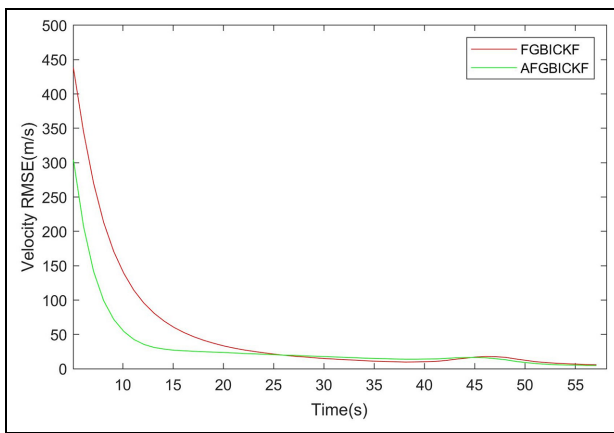


Figure 11. RMSEs in velocity for FGBICKF and AFGBICKF.

The initial information matrix (J_0) is calculated as:

$$J_0 = E\{-\Delta_{x_0}^x \log p(x_0)\} \quad (78)$$

Here, $\nabla_x = [\partial/\partial x_1, \partial/\partial x_2, \dots, \partial/\partial x_n]$ and $\Delta_x^x = \nabla_x \nabla_x^T$.

Next, we compare the STD of FGBICKF with PCRLB, as shown in Figure 9. Here, the values of the parameters (λ_1 , α , \hat{x}_0 , P_0 , Q_k , and R_k) are selected the same as those in the first subsection.

From the Figure 9(a) to (g), we see that the standard deviations of the position, velocity, and ballistic coefficient of FGBICKF are smaller than that of CKF and ICKF, and they are very close to PCRLB. These results further prove that FGBICKF is a state estimation algorithm with better performance.

Comparison of FGBICKF and AFGBICKF. In the simulation, the values of parameters (λ_1 , α , \hat{x}_0 , P_0 , Q_k , and R_k) are set the same as those in the first subsection. Figures 10 to 12 present RMSEs in position, velocity and ballistic coefficient for FGBICKF and AFGBICKF when the initial process noise covariance is $Q_0 = 1000 * Q_k$.

We see the obvious difference on the performance between the FGBICKF and AFGBICKF. Figures 10 to 12 shows that AFGBICKF keeps converging and its

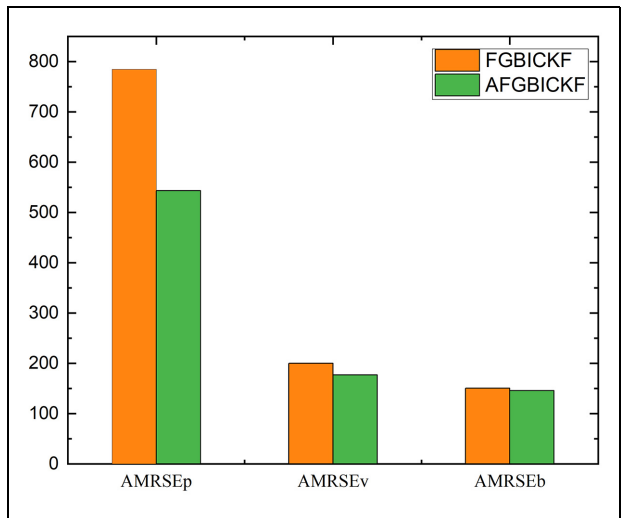


Figure 13. AMSREs for FBCICKF and AFGBICKF.

performance is better than that of FGBICKF. The simulation results prove that AFGBICKF can suppress the influence of the initial process noise covariance on state estimation.

Moreover, we compute the $AMSRE_p$, $AMSRE_v$ (AMSRE in velocity), and $AMSRE_b$ (AMSRE in ballistic coefficient) for FGBICKF and AFGBICKF, respectively, as shown in Figure 13.

From Figure 13, we can see that AFGBICKF has achieved comparable estimation accuracy to FGBICKF. The simulation results have demonstrated the prominent improvement over FGBICKF because the AFGBICKF incorporates the recursive procedures of estimating the process noise covariance.

AFGBICKF's adaptiveness to initial process noise covariance. In the simulation, the values of the parameters (λ_1 , α , \hat{x}_0 , P_0 , and R_k) are set the same as those in the first subsection and initial process covariance $Q_0 = Q_k$. Figures 14 to 16 present RMSEs in position, velocity and the

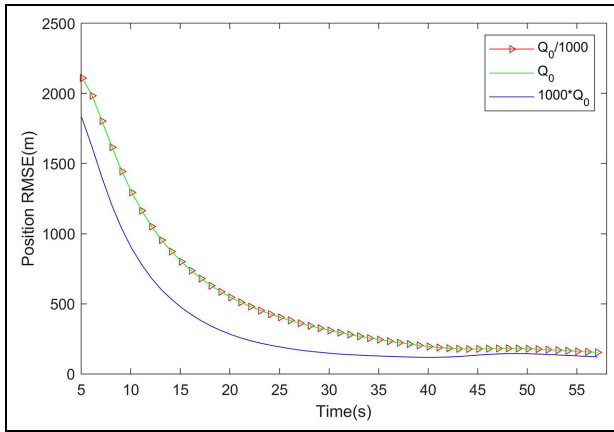


Figure 14. Position RMSE for AFGBICKF with various initial process noise covariances.

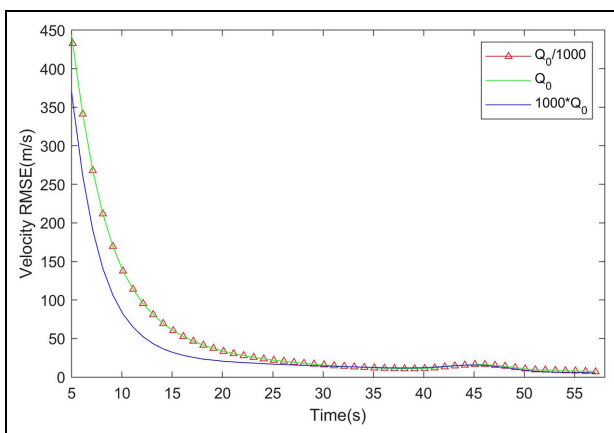


Figure 15. Velocity RMSE for AFGBICKF with various initial process noise covariances.

ballistic coefficient using the AFGBICKF algorithm when the initial process noise covariances are set to $Q_0/1000$, Q_0 , and $1000 * Q_0$, respectively.

From Figures 14 to 16, we can see that when the initial process noise covariance changes in a big range, from being small ($1/1000$ of Q_0) to big (1000 times of Q_0), AFGBICKF always converges and achieves almost same estimation performance. This validates the superiority of AFGBICKF and the correctness of our theoretical analysis in section 3.2. Moreover, a bigger initial estimate of process noise covariance gives better estimation performance. Thus, when accurate statistic of the process noise is unknown, a larger initial value is recommended to ensure the stability and convergence of filtering algorithms.

Conclusion

This paper proposes a novel filter FGBICKF to estimate the states for SNDS with Gaussian noise. Utilizing the fractional order gain, we further develop the FGBICKF with recursive process noise covariance estimation. FGBICKF uses fractional derivative of previous filter gains as feedback to current filter gain for

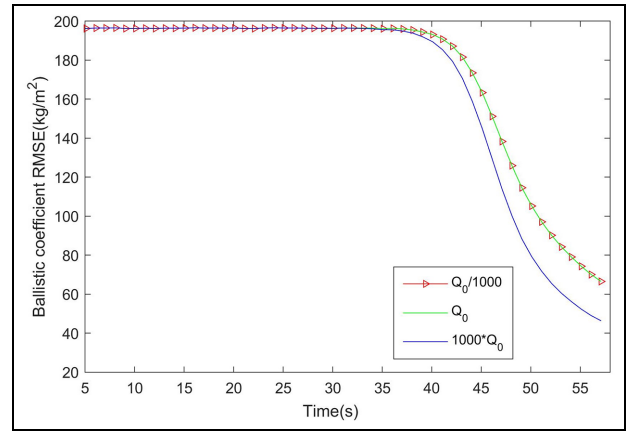


Figure 16. Ballistic coefficient RMSE for AFGBICKF with various initial process noise covariances.

estimating next states. The simulations on RBT tracking have proven FGBICKF’s superior estimation performance. Meanwhile, we have computed the PCRLB and compared it with relevant standard deviations of different filters, proving the effectiveness of FGBICKF. Moreover, the application of AFGBICKF to RBT tracking problem with unknown process noise covariance has shown AFGBICKF’s adaptiveness even when the initial process noise covariance changes dramatically. However, FGBICKF has some limitations. Firstly, the accuracy of the proposed filters depends on the accuracy of the system dynamics and measurement process. If the model does not accurately represent the real system, the filter’s estimates may deviate significantly from true states. Secondly, as the dimensionality of state increases, the matrix operations involved in the calculations become computationally intensive and require significantly additional computational resources. In the future, we will continue our research on addressing these limitations to estimate the states for SNDS more accurately and robustly.

Declaration of conflicting interests

The author(s) declared no potential conflicts of interest with respect to the research, authorship, and/or publication of this article.

Funding

The author(s) disclosed receipt of the following financial support for the research, authorship, and/or publication of this article: This work is supported by National Natural Science Foundation of China under grant number (No.62177037), Education Department of Shaanxi Provincial Government Service Local Special Scientific Research Plan Project under grant number (No.22JC037), and Key Science and Technology Program of Shaanxi Province under grant number (No.2019GY-067).

Availability of data and material

The data that support the findings of this study are available from the corresponding author upon reasonable request.

Compliance with ethical standards

Conflicts of interest The authors declare that they have no conflict of interests.

ORCID iD

Jing Mu  <https://orcid.org/0000-0002-7098-4434>

References

- Kalman RE. A new approach to linear filtering and prediction problems. *J Basic Eng* 1960; 82: 35–45.
- Mehra RK. Approaches to adaptive filtering. *IEEE Trans Automat Contr* 1972; 17: 693–698.
- Juler SJ and Uhlmann JK. Unscented filtering and nonlinear estimation. *Proc IEEE* 2004; 92: 401–422.
- Arasaratnam I and Haykin S. Cubature kalman filters. *IEEE Trans Automat Contr* 2009; 54: 1254–1269.
- Qiu ZB and Guo L. Improved cubature Kalman filter for spacecraft attitude estimation. *IEEE Trans Instrum Meas* 2021; 70: 1–13.
- Fang X and Huang D. Robust adaptive cubature Kalman filter for tracking manoeuvring target by wireless sensor network under noisy environment. *IET Radar Sonar Navig* 2023; 17(2): 179–190.
- Zhang Y, Huang Y, Li N, et al. Interpolatory cubature Kalman filters. *IET Control Theory Appl* 2015; 9: 1731–1739.
- Ma H, Zhang X, Lu Z, et al. An improved central difference Kalman filter for satellite attitude estimation with state mutation. *Int J Robust Nonlinear Control* 2022; 32: 3442–3468.
- Wilson KC. An optimal control approach to designing constant gain filters. *IEEE Trans Aerosp Electron Syst* 1972; AES-8: 836–842.
- Rao SK. Modified gain extended Kalman filter with application to bearings-only passive manoeuvring target tracking. *IEE Proc Radar Sonar Navig* 2005; 152: 239–244.
- Xu T, Zhu X and Zhang X. Infrared imaging Maneuvering Reentry Vehicle counter target lost algorithm using Modified Gain Extended Kalman Filter. In: *International Conference on Electronics, Communications and Control (ICECC)*, Ningbo, China, 9–11 September 2011, pp.1507–1511. New York, NY: IEEE.
- Chernoguz N. Adaptive-gain tracking filters based on minimization of the innovation variance. In: *IEEE international conference on acoustics speech and signal processing proceedings*, Toulouse, France, 14–19 May 2006, pp.III–III. New York, NY: IEEE.
- Liu C, Shui P, Wei G, et al. Modified unscented Kalman filter using modified filter gain and variance scale factor for highly maneuvering target tracking. *J Syst Eng Electron* 2014; 25: 380–385.
- Wang S, Feng J and Tse CK. Analysis of the characteristic of the Kalman gain for 1-D chaotic maps in cubature Kalman filter. *IEEE Signal Process Lett* 2013; 20: 229–232.
- Rashedi M, Liu J and Huang B. Distributed adaptive high-gain extended Kalman filtering for nonlinear systems. *Int J Robust Nonlinear Control* 2017; 27: 4873–4902.
- Mohamed AH and Schwarz KP. Adaptive Kalman filtering for INS/GPS. *J Geod* 1999; 73: 193–203.
- Zhu H, Zhang GR, Li YF, et al. An adaptive Kalman filter with inaccurate noise covariances in the presence of outliers. *IEEE Trans Automat Contr* 2022; 67: 374–381.
- Assa A and Plataniotis KN. Adaptive Kalman Filtering by Covariance Sampling. *IEEE Signal Process Lett* 2017; 24: 1288–1292.
- Wang H, Deng Z, Feng B, et al. An adaptive Kalman filter estimating process noise covariance. *Neurocomputing* 2017; 223: 12–17.
- Chang GB, Chen C, Zhang QZ, et al. Variational Bayesian adaptation of process noise covariance matrix in Kalman filtering. *J Franklin Inst* 2021; 358: 3980–3993.
- Wang J and Hao G. Robust estimation algorithm based on prior probability statistics. *Int J Robust Nonlinear Control* 2021; 31: 7957–7970.
- Chi J, Qian C, Zhang P, et al. A novel ELM based adaptive Kalman filter tracking algorithm. *Neurocomputing* 2014; 128: 42–49.
- Akhlaghi S, Zhou N and Huang Z. Adaptive adjustment of noise covariance in Kalman filter for dynamic state estimation. In: *IEEE power & energy society general meeting*, Chicago, IL, 16–20 July 2017, pp.1–5. New York, NY: IEEE.
- Assa A, Janabi-Sharifi F and Plataniotis KN. Sample-based adaptive Kalman filtering for accurate camera pose tracking. *Neurocomputing* 2019; 333: 307–318.
- De Vivo F, Brandl A, Battipede M, et al. Joseph covariance formula adaptation to Square-Root Sigma-Point Kalman filters. *Nonlinear Dyn* 2017; 88: 1987–1987.
- Zhang Y, Huang Y, Li N, et al. Embedded cubature Kalman filter with adaptive setting of free parameter. *Signal Process* 2015; 114: 112–116.
- Tseng CH, Lin SF and Jwo DJ. Robust Huber-based cubature Kalman filter for GPS navigation processing. *J Navig* 2017; 70: 527–546.
- Sierociuk D and Dzielinski A. Fractional Kalman filter algorithm for the states, parameters and order of fractional system estimation. *Int J Appl Math Comput Sci* 2006; 16: 129–140.
- Torabi H, Pariz N and Karimpour A. A novel cubature statistically linearized Kalman filter for fractional-order nonlinear discrete-time stochastic systems. *J Vib Control* 2018; 24: 5880–5897.
- Liu T, Cheng S, Wei Y, et al. Fractional central difference Kalman filter with unknown prior information. *Signal Process* 2019; 154: 294–303.
- Ramezani A, Safarinejadian B and Zarei J. Fractional order chaotic cryptography in colored noise environment by using fractional order interpolatory cubature Kalman filter. *Trans Inst Meas Control* 2019; 41: 3206–3222.
- Ramezani A, Safarinejadian B and Zarei J. Novel hybrid robust fractional interpolatory cubature Kalman filters. *J Franklin Inst* 2020; 357: 704–725.
- Tripathi RP, Singh AK and Gangwar P. Innovation-based fractional order adaptive Kalman filter. *J Electr Eng-Elektrotechnicky Casopis* 2020; 71: 60–64.
- Kaur H and Sahambi JS. Vehicle tracking in video using fractional feedback Kalman filter. *IEEE Trans Comput Imaging* 2016; 2: 550–512.
- Gao Z. Cubature Kalman filters for nonlinear continuous-time fractional-order systems with uncorrelated and correlated noises. *Nonlinear Dyn* 2019; 96: 1805–1817.

36. Tichavsky P, Muravchik CH and Nehorai A. Posterior Cramer-Rao bounds for discrete-time nonlinear filtering. *IEEE Trans Signal Process* 1998; 46: 1386–1396.
37. Genz A and Keister BD. Fully symmetric interpolatory rules for multiple integrals over infinite regions with Gaussian weight. *J Comput Appl Math* 1996; 71: 299–309.
38. Arasaratnam I, Haykin S and Hurd TR. Cubature Kalman filtering for continuous-discrete systems: theory and simulations. *IEEE Trans Signal Process* 2010; 58: 4977–4993.
39. Jiang H and Cai Y. Adaptive fifth-degree cubature information filter for multi-sensor bearings-only tracking. *Sensors* 2018; 18: 3241–3259.
40. Mu J and Cai Y. Likelihood-based iteration square-root cubature Kalman filter with applications to state estimation of re-entry ballistic target. *Trans Inst Meas Control* 2012; 35: 949–958.
41. Farina A, Ristic B and Benvenuti D. Tracking a ballistic target: comparison of several nonlinear filters. *IEEE Trans Aerosp Electron Syst* 2002; 38: 854–867.
42. Bar-Shalom Y, Li XR and Kirubarajan T. *Estimation with applications to tracking and navigation*. New York, NY: John Wiley & Sons, 2001.
43. Mu J, Tian F, Wang C, et al. Adaptive Masreliez-Martin fractional interpolatory cubature Kalman filter with recursive noise estimation. *J Vib Control* 2023; 29(17–18): 3907–3924.
44. Zheg Y, Ozdemir O, Niu R, et al. New conditional posterior Cramér-Rao lower bounds for nonlinear sequential Bayesian estimation. *IEEE Trans Signal Process* 2012; 60: 5549–5556.